

# Scaling laws for flows of jammed frictionless granular materials between parallel plates

Michio Otsuki<sup>1,2,\*</sup>, Kiwamu Yoshii<sup>3,4</sup>

<sup>1</sup>Graduate School of Engineering Science, Osaka University, 1–3 Machikaneyama, Toyonaka, Osaka 560–8531, Japan

<sup>2</sup>Institute of Science and Engineering, Shimane University, 1060 Nishikawatsu-cho, Matsue, Shimane 690-8504, Japan

<sup>3</sup>Department of Physics, Nagoya University, Furo-cho, Chikusa-ku, Nagoya 464–8602, Japan

<sup>4</sup>Department of Applied Physics, Tokyo University of Science, 6-3-1, Nijuku, Katsushika-ku, Tokyo 125–8585, Japan

**Abstract.** We theoretically study the flows of jammed frictionless granular materials driven by an external force between parallel plates. Using a continuum model, we analytically derive a scaling law that characterizes the critical behavior of the mass flux. When the external force is below a critical threshold, the mass flux remains zero, while it increases above this threshold, following a power-law dependence on the distance from the critical point. This scaling law is numerically verified using the discrete element method.

## 1 Introduction

Granular materials exhibit a wide range of behaviors depending on the packing fraction  $\phi$  [1]. When  $\phi$  exceeds the jamming transition point  $\phi_J$ , they behave as solids, while for  $\phi < \phi_J$ , they flow like fluids. This rheological transition, known as the jamming transition, is commonly observed in disordered materials such as colloidal suspensions, foams, and emulsions [2]. Jammed granular materials act as linear elastic solids under sufficiently small shear stress  $\tau$ , but they begin to flow with a nonzero shear rate  $\dot{\gamma}$  when  $\tau$  exceeds the yield stress. Jamming in granular materials frequently occurs in industrial processes. Therefore, it has been widely studied in recent years [3].

In disordered materials near  $\phi_J$ , physical quantities such as pressure, shear modulus, and coordination number exhibit critical power-law behavior [3]. Under uniform shear, the shear stress  $\tau$  and pressure  $p$ , which depend on  $\phi$  and  $\dot{\gamma}$ , follow critical scaling laws [4]. These critical behaviors have been primarily investigated in homogeneous systems, where  $\phi$  and  $\dot{\gamma}$  are spatially uniform. However, in manufacturing processes such as hoppers, sand piles, and rotating drums [5], jamming typically occurs in inhomogeneous systems, raising the question of whether the critical scaling laws established for homogeneous systems remain applicable.

To investigate the critical behavior in inhomogeneous systems, a previous study has examined granular flow between rough parallel plates driven by an external force  $f$  [6]. The mass flux  $Q$ , which characterizes the flow, remains zero when  $f$  is below a critical force  $f_c$  and increases once  $f$  exceeds  $f_c$ . Using a continuum model based on the constitutive equation known as  $\mu(I)$ -rheology [7], a critical scaling law for  $Q$  has been analytically de-

rived and verified through numerical simulations using the discrete element method (DEM).

The  $\mu(I)$ -rheology, originally proposed for homogeneous steady flows [8], describes the local bulk friction  $\mu = |\tau|/p$  in terms of the local inertial number  $I = |\dot{\gamma}|d/\sqrt{p/\rho_s}$ , where  $\rho_s$  is the grain material density and  $d$  is the mean grain diameter:

$$\mu = \mu_{\text{loc}}(I) = \mu_s + \frac{\mu_2 - \mu_s}{I_0 I + 1}. \quad (1)$$

Here,  $\mu_s$ ,  $\mu_2$ , and  $I_0$  are dimensionless parameters. However, recent studies have shown that the local  $\mu(I)$ -rheology fails to capture creep flow in inhomogeneous systems due to nonlocal effects [9–11]. Therefore, the validity of the critical scaling law derived from the local  $\mu(I)$ -rheology needs to be reassessed carefully.

In this paper, we analytically investigate granular flows between parallel plates based on a continuum model that incorporates the nonlocal effect. In Sec. 2, we derive the velocity profile and demonstrate that the scaling law obtained from the local  $\mu(I)$  rheology becomes valid when the plate separation is sufficiently large. In Sec. 3, we numerically verify the scaling law using DEM simulations. Finally, we discuss and conclude our results in Sec. 4.

## 2 Theoretical analysis

### 2.1 Setup for theoretical analysis

We consider the two-dimensional flow of frictionless grains with identical density  $\rho_s$  between parallel plates, as shown in Fig. 1. The plates are rough, aligned parallel to the  $x$ -direction, and positioned at  $z = \pm H/2$ . The distance between the plates is denoted by  $H$ . The interaction between grains is modeled using a linear spring-dashpot model [6]. The grains are driven by an external force  $f$

\*e-mail: m.otsuki.es@osaka-u.ac.jp

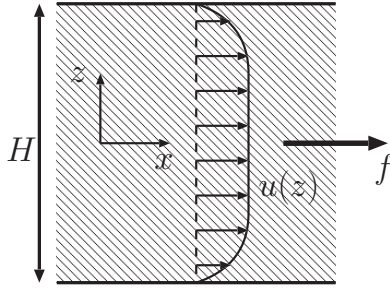


**Figure 1.** Schematic of granular flow between rough parallel plates, showing the configuration, direction of the applied force, and the general profile of the velocity field  $u(z)$ .

per unit mass along the  $x$ -direction, which induces a steady flow characterized by the velocity profile  $u(z)$  along the  $x$ -direction.

We now examine the case where the spatially averaged packing fraction  $\phi_0$  is greater than  $\phi_J$ . For  $\phi_0 > \phi_J$ , the velocity  $u(z)$  remains zero throughout the entire system if the external force is below a critical force  $f_c$ , which depends on  $\phi_0$  and  $H$ . In contrast, for  $f > f_c$ , the granular materials exhibit flow, satisfying  $u(z) > 0$  for  $|z| < H/2$  [6]. Due to the symmetry of the system, the velocity profile satisfies  $u(z) = u(-z)$ .

We focus on the critical behavior of the steady flow near  $f_c$  for a sufficiently large system with  $d/H \ll 1$ . For  $f \sim f_c$ , the packing fraction and pressure are approximated as  $\phi_0$  and  $p(\phi_0) = B(\phi_0 - \phi_J)$ , respectively, for all  $z$ , where  $B$  is a constant, which are perturbatively derived using a continuum model in Ref. [6]. Under steady flow conditions, the shear stress  $\tau(z)$  satisfies the momentum conservation equation:

$$\frac{d\tau(z)}{dz} = -\rho_s \phi_0 f. \quad (2)$$

In Ref. [6], the shear rate

$$\dot{\gamma}(z) = \frac{du(z)}{dz} \quad (3)$$

and the velocity profile  $u(z)$  have been derived from the shear stress  $\tau(z)$  satisfying Eq. (2) and the local  $\mu(I)$ -rheology given by Eq. (1). However, in this study, we adopt a nonlocal constitutive model proposed in Ref. [9].

In this constitutive model, the granular fluidity  $g(z)$  is introduced, which gives the shear rate  $\dot{\gamma}(z)$  as [9]

$$|\dot{\gamma}(z)| = \mu(z)g(z), \quad g(z) = g_{\text{loc}}(z) + \xi^2(z) \frac{d^2}{dz^2} g(z). \quad (4)$$

with  $\mu(z) = |\tau(z)|/p$ . Note that, in the case of emulsions, the relation between  $\dot{\gamma}$  and  $\tau$  is described in terms of the fluidity within a nonlocal constitutive model [9]. Here,  $g_{\text{loc}}(z)$  is the local fluidity given by [10]

$$g_{\text{loc}}(z) = \Theta(\mu(z) - \mu_s) \sqrt{\frac{p}{\rho_s} \frac{I_0}{d}} \frac{\mu(z) - \mu_s}{\mu(z)(\mu_2 - \mu(z))}, \quad (5)$$

with the Heaviside function  $\Theta(x)$ , and  $\xi(z)$  is the cooperativity length given by [11]

$$\xi(z) = Ad / \sqrt{|\mu(z) - \mu_s|} \quad (6)$$

with a dimensionless parameter  $A$ . At the parallel plates ( $z = \pm H/2$ ), we set  $g = g_{\text{loc}}$  following Ref. [9]. It should be noted that when  $\xi$  is approximately neglected in Eq. (4),  $g(z)$  approaches  $g_{\text{loc}}(z)$ , and the constitutive equation simplifies to the local  $\mu(I)$ -rheology (Eq. (1)). However,  $\xi$  diverges as  $\mu \rightarrow \mu_s$ . Therefore, this approximation requires careful treatment.

## 2.2 Shear Rate

Due to the symmetry of  $u(z)$ , we find  $\dot{\gamma}(z) = \tau(z) = 0$  at  $z = 0$ . Using this condition and Eq. (2), we obtain  $\tau(z) = \rho_s \phi_0 f z$ , which gives

$$\mu(z) = |\tau(z)|/p = \rho_s \phi_0 f |z|/p. \quad (7)$$

In the static state, where  $u(z) = \dot{\gamma}(z) = 0$  throughout the system, we have  $g_{\text{loc}}(z) = 0$  and  $\mu(z) < \mu_s$ . From Eq. (7),  $\mu(z)$  is largest at  $z = \pm H/2$ , which provides the condition for the static state:

$$f < f_c \equiv 2\mu_s p / (\rho_s \phi_0 H). \quad (8)$$

Here,  $f_c$  is the critical force.

To obtain the velocity profile  $u(z)$  for  $f \geq f_c$ , we introduce the size of the region where  $\mu(z) \geq \mu_s$ , which is given by  $\ell = (H/2)(\epsilon/(1 + \epsilon))$  with

$$\epsilon = (f - f_c)/f_c. \quad (9)$$

Here,  $\epsilon$  represents the deviation from the critical force  $f_c$ . We divide the system into two regions:  $|z| < H/2 - \ell$  and  $H/2 - \ell \leq z$ . We then introduce the normalized position in each region as

$$\zeta_+(z) = \{|z| - (H/2 - \ell)\}/\ell, \quad (10)$$

$$\zeta_-(z) = \{(H/2 - \ell) - |z|\}/(H/2 - \ell). \quad (11)$$

With the introduction of  $\zeta_{\pm}(z)$ , we express  $\mu(z)$  in Eq. (7) as

$$\mu(z) - \mu_s = \begin{cases} \mu_s \epsilon \zeta_+(z), & H/2 - \ell \leq |z|, \\ -\mu_s \zeta_-(z), & |z| < H/2 - \ell. \end{cases} \quad (12)$$

Substituting Eq. (12) into Eqs. (5) and (6), we obtain

$$g_{\text{loc}}(z) = \begin{cases} \sqrt{\frac{p}{\rho_s} \frac{I_0}{d}} \frac{\epsilon}{\mu_2 - \mu_s} \zeta_+(z), & H/2 - \ell \leq |z|, \\ 0, & |z| < H/2 - \ell, \end{cases} \quad (13)$$

and

$$\xi(z) = \begin{cases} A^2 d^2 / (\mu_s \epsilon \zeta_+(z)), & H/2 - \ell \leq |z|, \\ A^2 d^2 / (\mu_s \zeta_-(z)), & |z| < H/2 - \ell. \end{cases} \quad (14)$$

Here, we have approximated  $\mu(z) = \mu_s(1 + \epsilon \zeta_{\pm}(z)) \approx \mu_s$  for  $H/2 - \ell \leq |z|$ , as we consider the case near  $f_c$  ( $\epsilon \ll 1$ ).

We represent  $g(z)$  using  $\zeta_{\pm}(z)$  as

$$g(z) = \sqrt{\frac{p}{\rho_s} \frac{I_0}{d}} \frac{\epsilon}{\mu_2 - \mu_s} F(z) \quad (15)$$

with

$$F(z) = \begin{cases} \zeta_+(z) + \Gamma_+(\zeta_+(z)), & H/2 - \ell \leq |z|, \\ \Gamma_-(\zeta_-(z)), & |z| < H/2 - \ell. \end{cases} \quad (16)$$

Substituting Eqs. (13), (14), (15), and (16) along with Eqs. (10) and (11) into Eq. (4), we find  $\Gamma_{\pm}(\zeta)$  satisfies

$$\zeta \Gamma_{\pm}(\zeta) = \alpha_{\pm}^3 \frac{d^2}{d\zeta^2} \Gamma_{\pm}(\zeta) \quad (17)$$

with  $\alpha_+ = (A^2/\mu_s)^{1/3} (1 + \epsilon)^{2/3} \epsilon^{-1} (2d/H)^{2/3}$  and  $\alpha_- = \epsilon\alpha_+$ . It should be noted that  $\alpha_{\pm}$  converges to 0 for sufficiently large system with  $d/H \rightarrow 0$ . From the boundary conditions  $g = g_{\text{loc}}$  at  $\zeta = 1$  ( $z = \pm H/2$ ) and continuity of  $g$  at  $\zeta = 0$  ( $z = H/2 - \ell$ ),  $\Gamma_{\pm}(\zeta)$  satisfy  $\Gamma_{\pm}(\zeta = 1) = 0$ ,  $\Gamma_+(0) = \Gamma_-(0)$ , and  $\Gamma'_+(0) = \Gamma'_-(0)$ . The solution of Eq. (17) satisfying these conditions is given by

$$\Gamma_{\pm}(\zeta) = \alpha_{\pm} \frac{E_{\pm}}{E_+F_- + E_-F_+} \Psi_{\pm}(\zeta) \quad (18)$$

with  $\Psi_{\pm}(\zeta) = \text{Ai}(\zeta/\alpha_{\pm}) \text{Bi}(1/\alpha_{\pm}) - \text{Ai}(1/\alpha_{\pm}) \text{Bi}(\zeta/\alpha_{\pm})$  and  $E_{\pm} = \Psi_{\pm}(\zeta = 0)$ ,  $F_{\pm} = \alpha_{\pm} \Psi'_{\pm}(\zeta = 0)$ . Here,  $\text{Ai}(x)$  and  $\text{Bi}(x)$  are the Airy functions of the first and second kind.

With Eqs. (4), (15), and (16), we obtain

$$\dot{\gamma}(z) = \begin{cases} \sqrt{\frac{p}{\rho_s} \frac{I_0}{d} \frac{\mu(z)\epsilon}{\mu_2 - \mu_s}} (\zeta_+(z) + \Gamma_+(\zeta_+(z))), & H/2 - \ell \leq |z| \\ \sqrt{\frac{p}{\rho_s} \frac{I_0}{d} \frac{\mu(z)\epsilon}{\mu_2 - \mu_s}} \Gamma_-(\zeta_-(z)), & |z| < H/2 - \ell. \end{cases} \quad (19)$$

The nonlocal effect associated with the slow creep motion is represented by  $\Gamma_{\pm}(\zeta)$ , because the shear rate  $\dot{\gamma}$  is nonzero even in the region with  $\mu < \mu_s$  ( $|z| < H/2 - \ell$ ) if  $\Gamma_{\pm}(\zeta) \neq 0$ . The function  $\Gamma_{\pm}(\zeta)$  given by Eq. (18) is a decreasing function for  $0 \leq \zeta \leq 1$  satisfying  $0 \leq \Gamma_{\pm}(\zeta) \leq \alpha_{\pm}\chi$  with  $\chi = E_+E_-/(E_+F_- + E_-F_+)$ . A similar solution is also derived in Ref. [11], but the critical behavior near  $f_c$  has not been discussed.

### 2.3 Velocity profile and mass flux

Here, we consider a sufficiently large system with  $d/H \rightarrow 0$ . In the limit  $d/H \rightarrow 0$ , the maximum value of  $\Gamma_{\pm}(\zeta)$  converges to  $\alpha_{\pm}\chi \rightarrow \alpha_{\pm} |\text{Ai}(0)/\text{Ai}'(0)| \sim O((H/d)^{2/3})$ . Hence, in the limit of a sufficiently large distance with  $d/H \rightarrow 0$  for a given  $\epsilon$ , we can neglect the nonlocal effect,  $\Gamma_{\pm}(\zeta)$ , in Eq. (19) and obtain

$$|\dot{\gamma}(z)| = \Theta(|z| + H/2 - \ell) \sqrt{\frac{p}{\rho_s} \frac{I_0}{d} \frac{\mu_s \epsilon}{\mu_2 - \mu_s}} \zeta_+(z), \quad (20)$$

where we have also neglected the higher-order terms of  $\epsilon$  for  $\epsilon \ll 1$ . Integrating Eq. (3) with respect to  $z$  and using Eq. (20) and the boundary conditions ( $u(z = \pm H/2) = 0$ ), we obtain the velocity profile as

$$u(z) = \begin{cases} U_M |1 - \zeta_+(z)|^2, & H/2 - \ell \leq |z| \\ U_M, & |z| < H/2 - \ell. \end{cases} \quad (21)$$

with

$$U_M = \frac{\mu_s I_0}{4(\mu_2 - \mu_s)} \sqrt{\frac{p}{\rho_s} \frac{H}{d}} \Theta(\epsilon) \epsilon^2, \quad (22)$$

which is consistent with the velocity profile obtained using the local  $\mu(I)$ -rheology [6]. In Eq. (22),  $\Theta(\epsilon)$  indicates that the flow stops for  $f < f_c$  ( $\epsilon < 0$ ). The mass flux  $Q$  is obtained from Eqs. (21) and (22) with  $Q = \int_{-H/2}^{H/2} dz \rho_s \phi_0 u(z)$  as

$$Q = \frac{\mu_s I_0 \rho_s \phi_0}{4(\mu_2 - \mu_s)} \sqrt{\frac{p}{\rho_s} \frac{H^2}{d}} \Theta(\epsilon) \epsilon^2, \quad (23)$$

where we have neglected the higher-order terms  $O(\epsilon^3)$ .

Substituting Eq. (9) into Eq. (23) with Eq. (8), we obtain the following scaling law for  $Q$ :

$$Q = \frac{I_0 \rho_s \phi_0 d^3}{16 \mu_s (\mu_2 - \mu_s)} \left( \frac{p(\phi_0)}{\rho_s} \right)^{3/2} \left( \frac{H}{d} \right)^4 (f - f_c(\phi_0, H))^2 \quad (24)$$

for  $f \geq f_c$ , while  $Q = 0$  for  $f < f_c$ . This equation shows that the square root of the mass flux,  $\sqrt{Q}$ , increases linearly with  $f$  above  $f_c$ , with the slope being proportional to  $H^2$ . Note that while there are many studies on scaling laws for granular flows on inclined planes [5, 12], the critical scaling behavior near jamming has not been addressed.

### 3 Numerical verification

In Ref. [6], Eq. (24) has been derived from the local  $\mu(I)$ -rheology, and the critical scaling law near  $\phi_0$ , obtained by using the  $\phi_0$ -dependence of  $p$ , has been numerically verified. However, the dependence of  $Q$  on  $f$  has not been discussed in detail. Therefore, in this subsection, we investigate  $Q$  as a function of  $f$  for a given  $\phi_0$  using DEM simulations.

In these simulations, granular materials, as shown in Fig. 1, consist of an equal number of particles with diameters  $d_0$  and  $sd_0$  with  $s = 1.4$ . The mean diameter is given by  $d = (1 + s)d_0/2$ . The interaction force, realized by the linear spring-dashpot model, is characterized by the elastic constant  $k$  and viscosity  $\eta$ . The rough parallel walls with length  $L$  are made of particles with diameter  $d_0$ , equally spaced at  $z = \pm H/2$ . The parameters are set as  $\phi_0 = 0.850$ ,  $L/d_0 = 200$ , and  $\eta/\sqrt{m_0 k} = 1$ , with  $m_0$  being the mass of a particle with diameter  $d_0$ . We use  $H/d_0 \geq 200$  to neglect the nonlocal effect, as assumed in our analytical calculations. The units of the external force and mass flux are denoted by  $f_0 = kd_0/m_0$  and  $Q_0 = \sqrt{m_0 k}$ , respectively. The details are provided in Ref. [6].

In Fig. 2(a), we plot  $\sqrt{Q}$  against  $f$  for  $H/d_0 = 200, 300, \text{ and } 400$ . The square root of  $Q$  increases linearly when  $f$  exceeds  $f_c$ , where  $f_c$  decreases with increasing  $H$ . The slope of  $\sqrt{Q}$  increases with  $H$ . These behaviors are consistent with our analytical results given by Eqs. (8) and (24).

From Eq. (24), we obtain a scaling law for  $\sqrt{Q}$  at a given  $\phi_0$  as

$$\sqrt{Q}/H^2 \propto f - f_c. \quad (25)$$

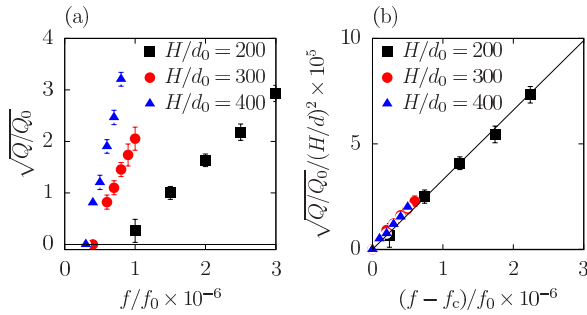


**Figure 2.** (a) Plot of  $\sqrt{Q}$  versus  $f$  for various values of  $H$ . (b) Scaling plot of  $\sqrt{Q}$  based on Eq. (25) for various values of  $H$ . The solid line represents  $\sqrt{Q}/H^2 \sim (f - f_c)$ .

In Fig. 2(b), we present the scaling plot of  $\sqrt{Q}$  based on Eq. (25). Here, we estimate  $f_c$  as the value of  $f$  at which  $Q$  exceeds  $10^{-4} Q_0 (H/d_0)^2$ . We observe excellent data collapse for various values of  $H$ , which verifies our analytical results given by Eq. (24).

## 4 Discussion and Conclusion

In this paper, we have theoretically and numerically shown that the nonlocal effect is negligible for the dependence of  $Q$  on  $f$  in the limit of  $d/H \ll 1$ . However, the nonlocal effect becomes significant for smaller values of  $H$  in the profiles of  $\dot{\gamma}(z)$  and  $u(z)$ , as shown in Ref. [6]. The dependence of the nonlocal effect on  $Q$  for smaller  $H$  will be addressed in future work.

We have numerically investigated the mass flux  $Q$  as a function of the external force  $f$ . Our system can be regarded as an assembly of disks on a slope with angle  $\theta$ , where  $f$  is given by  $G \sin \theta$  with the gravitational acceleration  $G$ . We introduced  $\epsilon$  as the nondimensionalized deviation from the critical force in Eq. (9), and it can also be written as  $\epsilon = (H - H_c)/H_c$  with  $H_c = (2\mu_s p)/(\rho_s \phi_0 f)$ . Here,  $H_c$  can be interpreted as the critical distance for a given  $f$ , where the flow occurs for  $H > H_c$ . Hence, Eq. (23) can be used to describe the critical behavior of the flow when varying the distance  $H$  between the plates.

It has been reported that the frictionless limit of the  $\mu$ - $I$  relation is singular for sufficiently small  $I$  [12]. While our study focuses on flows of frictionless grains, the influence of this singularity on the scaling laws remains to be addressed in future work.

In conclusion, we have theoretically investigated the velocity field of frictionless granular materials between parallel plates driven by an external force based on a continuum model. From the solution for the shear rate  $\dot{\gamma}(z)$ , we derived a scaling law for the mass flux  $Q$  in the limit of  $d/H \ll 1$ . This scaling law has been numerically verified using DEM simulations, confirming the consistency between the theoretical and numerical results. Our findings provide a deeper understanding of the flow behavior of granular materials under external forces.

The authors thank H. Hayakawa and T. Barker for their fruitful discussions. M.O. is partially supported by JSPS KAKENHI (Grants No.23K03248). K.Y. is partially supported by JSPS KAKENHI (Grants No.24KJ0110) and The Public Foundation of Chubu Science and Technology Center. K.Y. would like to thank the Research center for Computational Science, Okazaki, Japan for making its supercomputer system available (Project: 22-IMS-C267 and 23-IMS-C126).

## References

- [1] B. Andreotti, Y. Forterre, O. Pouliquen, *Granular Media; Between Fluid and Solid* (Cambridge University Press, Cambridge, 2013)
- [2] A.J. Liu, S.R. Nagel, Jamming is not just cool any more, *Nature* **396**, 21 (1998). <https://doi.org/10.1038/23819>
- [3] M. van Hecke, Jamming of soft particles: geometry, mechanics, scaling and isostaticity, *J. Phys. Condens. Matter* **22**, 033101 (2010). <https://doi.org/10.1088/0953-8984/22/3/033101>
- [4] P. Olsson, S. Teitel, Critical scaling of shear viscosity at the jamming transition, *Phys. Rev. Lett.* **99**, 178001 (2007). <https://doi.org/10.1103/PhysRevLett.99.178001>
- [5] G.D.R. MiDi, On dense granular flows, *Eur. Phys. J. E* **14**, 341 (2004). <https://doi.org/10.1140/epje/i2003-10153-0>
- [6] M. Otsuki, K. Hayashi, K. Yoshii, Critical scaling for dense granular flow between parallel plates near jamming (2024), arXiv:2403.00256. <https://doi.org/10.48550/arXiv.2403.00256>
- [7] P. Jop, Y. Forterre, O. Pouliquen, A constitutive law for dense granular flows, *Nature* **441**, 727 (2006). <https://doi.org/10.1038/nature04801>
- [8] F. da Cruz, S. Emam, M. Prochnow, J.N. Roux, F. Chevoir, Rheophysics of dense granular materials: Discrete simulation of plane shear flows, *Phys. Rev. E* **72**, 021309 (2005). <https://doi.org/10.1103/PhysRevE.72.021309>
- [9] K. Kamrin, G. Koval, Nonlocal constitutive relation for steady granular flow, *Phys. Rev. Lett.* **108**, 178301 (2012). <https://doi.org/10.1103/PhysRevLett.108.178301>
- [10] D. Liu, D.L. Henann, Non-local continuum modelling of steady, dense granular heap flows, *J. Fluid Mech.* **831**, 212 (2017). <https://doi.org/10.1017/jfm.2017.554>
- [11] D. Liu, D.L. Henann, Size-dependence of the flow threshold in dense granular materials, *Soft Matter* **14**, 5294 (2018). <https://doi.org/10.1039/C8SM00843D>
- [12] D. Dumont, H. Bonneau, T. Salez, E. Raphaël, P. Damman, Microscopic foundation of the  $\mu(i)$  rheology for dense granular flows on inclined planes, *Phys. Rev. Res.* **5** (2023). [10.1103/PhysRevResearch.5.013089](https://doi.org/10.1103/PhysRevResearch.5.013089)